

Development of an autonomous Global Navigation Satellite System ground station and its calibration for monitoring of local ionospheric perturbations

Roman Galas[✉], Marija Čokrić

Technische Universität Berlin, Department of Geodesy and Geoinformation Science
Straße des 17. Juni 135, 10623 Berlin, Germany, e-mails: {roman.galas; marija.cokric}@tu-berlin.de
[✉] corresponding author

Key words: local ionospheric perturbations, scintillations, single autonomous GNSS monitoring station, continuously monitoring GNSS ground systems, autonomous power management, real-time processing, hardware calibration

Abstract

A state-of-the-art monitoring global navigation satellite system (GNSS) system has been originally designed and developed for various positioning and atmosphere-sensing purposes by the authors and updated to fulfil the challenging requirements for monitoring of ionospheric perturbations. The paper discusses various scientific and technically challenging issues, such as the requirement for an autonomous operating ground GNSS station and how this can be fulfilled. Basic algorithms for monitoring of local ionospheric perturbations with GNSS receivers are described. The algorithms require that inter-frequency hardware biases be known. Although the satellite transmitter biases can be obtained from the IGS services, the user takes responsibility for the estimation of frequency dependent receiver hardware biases and for the control of their variations. The instrumental signal delays are important for timing applications and GNSS monitoring of the ionosphere and are also required for recovering of the integer carrier-phase ambiguities. The paper presents an algorithm for calibration of inter-frequency biases of global positioning system (GPS) receivers and validates the first set of results.

Introduction

The autonomous global positioning system (GPS) monitoring station presented in the paper is already one of the “next generation GPS real-time monitoring stations”. The first systems (the so called GPS arrays) were developed for ground surface deformations monitoring for volcanoes (Guntur in Indonesia or Popocatepetl in Mexico) (Galas R. et al., 2003).

The aim of our research and experiments was to investigate the applicability of GPS technology for early warning systems of natural hazards. Nevertheless the experiments are considered successful because the Popocatepetl array was operating, without on-site visits for system maintenance, over a period far exceeding one year. It was one of the first remotely operated GPS-based natural hazard warning prototype systems (Figure 1).

The main goal of the investigations presented here was the development of a reliable, autonomous and continuously operating GPS-based ground system that is able to provide 50 Hz GPS data for monitoring of local ionospheric irregularities in a real time mode, to support geoscientists and surveyors and to contribute to space weather systems.

In global navigation satellite system (GNSS) precise positioning, it is crucial to support the users with reliable ionospheric maps. First order ionospheric variations can be characterised with the parameter TEC (total electron content). The TECs describe variations in time and in space state of the ionosphere. Regular variations of the ionosphere occur in periodical cycles and can be modelled and predicted. The GPS ground monitoring stations provide ground measurements of the slant TEC (sTEC: the TEC integrated value along the signal path).



Figure 1. The low-latency/high-rate GNSS operating station on Popocatepetl (The laptop computer is used only for maintenance. It is not a part of the station equipment)

From the ionospheric models, the so call vertical TEC (vTEC) can be obtained as a function of time and geographical coordinates. Irregular ionospheric variations, especially the local ones, are random and difficult or even impossible to predict. However, for some critical real-time GPS positioning (navigation) applications and for trans-ionospheric communication systems, it might be useful to support the users with broadcast messages about local ionospheric disturbances. Very well-known phenomena caused by the variability of the TEC are travelling ionospheric disturbances (TIDs) and ionospheric scintillations. Both phenomena can be detected in sTEC time series, which can be estimated relatively easy using precise multi-frequency GNSS receivers. The importance of real time information about the state of the ionosphere cannot be underestimated. The aim of the presented investigations was the development of hardware and a software system for critical and challenging applications of local monitoring of the ionosphere with ground GNSS stations. It was also investigated how far a singular GNSS-based ionosphere monitoring station can contribute to geodetic applications.

Estimation of TEC values at a single station using a dual frequency GNSS receiver

The primary observables used for TEC reconstructions are code- (P_i) and carrier-phase (L_i) observables. The subscript i describes the frequency number.

Variations in the value of the sTEC can be estimated directly from dual frequency GPS observables

using the following equation (Klobuchar, 1996; p. 489) expressing the influence of the first order term of the ionospheric delay [s]:

$$\Delta t_{g,f_i} = -\Delta t_{ph,f_i} = \frac{1}{c} \frac{A}{2f_i^2} \text{sTEC} \quad [s] \quad (1)$$

where:

g, ph – group- and carrier-phase delays, respectively;

f_i – frequency of the carrier wave;

c – the speed of light;

$A = 80.6 \text{ m}^3 \text{ s}^{-2}$ (Hartmann & Leeitinger, 1984);

sTEC – the total electron content integrated along the signal path from satellite S to receiver R

$$\int_R^S N_e ds, \text{ expressed in the TEC units (TECU, } 1 \text{ TEC} = 10^{16} [\text{e}\cdot\text{m}^{-2}]).$$

From the above, the difference of the ionospheric delays between two waves with frequencies f_1, f_2 , follows:

$$\delta \Delta t_{g,f_1-f_2} = \frac{40.30}{c} \frac{f_2^2 - f_1^2}{f_1^2 f_2^2} \text{sTEC} \quad [s] \quad (2a)$$

and

$$\delta \Delta t_{ph,f_1-f_2} = -\frac{40.30}{c} \frac{f_2^2 - f_1^2}{f_1^2 f_2^2} \text{sTEC} \quad [s] \quad (2b)$$

where $\delta \Delta t_{g,f_1-f_2}$ and $\delta \Delta t_{ph,f_1-f_2}$ are ionospheric slant delays estimated from code- and carrier-phase measurements, respectively.

Using in situ measurements of ionospheric delays $\delta \Delta t_{g,f_1-f_2}$ from radio receivers, the above equations allow the estimation of variations in time of the sTEC values (first order term). Those data can

be used, among others, for generation of ionospheric models, monitoring of local ionospheric disturbances and issuing of warning messages for users of navigation- and communication trans-ionospheric systems.

The ionospheric delay terms ($\delta\Delta t_{g,f1-f2}$ and $\delta\Delta t_{ph,f1-f2}$) in both equations above can easily be estimated using GNSS “geometry free” (called also “ionospheric”) secondary observables (expressed in meters) derived from the primary code-

$$(\delta\Delta t_{g,f1-f2}) = \frac{1}{c} P_{GF,R}^S = \frac{1}{c} (P_{1,R}^S - P_{2,R}^S) \quad [s] \quad (3a)$$

and carrier-phase measurements

$$(\delta\Delta t_{ph,f1-f2}) = -\frac{1}{c} L_{GF,R}^S = \frac{1}{c} (L_{2,R}^S + L_{1,R}^S) \quad [s] \quad (3b)$$

The sampling rate of the GPS observables should be at least 1 Hz (better 10 Hz or even 50 Hz). Some auxiliary observables for monitoring of the state of the ionosphere are needed as well. The most important are I- and Q-amplitudes (correlations) for estimation of the amplitude scintillation index S4. The I/Qs should be provided with the sampling rate of 50 Hz.

The measurements on the right side of the above equations (3) are biased by unknown between-frequencies hardware (instrumental) delays, which must be calibrated. An algorithm for calibration of the receiver inter-frequency instrumental delays will be presented below.

A GNSS-based ground station for monitoring of the ionosphere

Our GNSS station for monitoring of the ionosphere is to be located in the polar cup and/or in equatorial areas. Both locations are of great interests, because ionospheric disturbances are much stronger there than at mid-latitudes, and due to this can provide valuable experimental data for studies of ionospheric impacts on trans-ionospheric communication and navigation systems.

The system design is based on our earlier developments for volcano monitoring GPS arrays, GPS-buoys for altimetry calibration, ground networks for the satellite CHAMP mission and tsunami warning systems, among others. It is equipped with an uninterrupted self-controlling power supply sub-system and reliable station computers. It can be maintained remotely from a distant control site without intensive maintenance on the site, which fulfils the most critical requirement for GNSS continuous tracking

stations. There are no mechanical items, and the system can be operated in a broad temperature range of -20°C to $+50^{\circ}\text{C}$. The implemented uninterrupted power supply ensures that the station will operate autonomously over a period of ~ 4 days, and there is enough data storage capacity on site to archive at least two weeks of raw data (a ring buffer).

In case of longer power-off periods, the station system enters a “sleeping mode”. In sleeping mode, the system recognizes whether the batteries are re-charged. In such a case, the control data unit (CDU) is automatically switched on and the following actions are performed: a) the sensors are switched on and configured, b) the software tools for recording of sensor-measurements, data transmission and data archiving are invoked. The CDU is based on a PC-104 single board computer with stable Linux operating system based on the SUSE distribution v. 7.3. installed on a PCMCIA flash memory card.

The most critical software modules are data-loggers. Our GPS data logger for Septentrio PolaRxS receivers can store 50 Hz data (primary and auxiliary observables). Other software applications are a) GPS-daemon, invoking and monitoring all station processes, b) battery manager, c) shell scripts for data archiving.

Calibration of the inter-frequency hardware biases: mathematical models and algorithm

The algorithm is based on equations (3a) and (3b). The ionospheric term will be derived from the GPS primary code- and carrier-phase phase observables. The observables used here are: $P_{f,R}^S$ and $L_{f,R}^S$. Observational models for the primary GNSS observables (pseudo-ranges between satellite S and receiver R) can be found in a number of text-books on satellite geodesy (e.g. Hofmann-Wellenhof, Lichtenegger & Wasle, 2008) and are not discussed here. Derived from them, geometry free (ionospheric) code- ($P_{GF,R}^S$) and carrier- ($L_{GF,R}^S$) phase observables (in [m]) can be modelled as below:

$$P_{GF,R}^S = (\delta\Delta t_{g,f1-f2})c = \left(1 - \frac{f_1^2}{f_2^2}\right) I_{1,R}^S + (\beta_1^S - \beta_2^S) + (\beta_{1,R} - \beta_{2,R}) \quad (4a)$$

$$L_{GF,R}^S = -(\delta\Delta t_{ph,f1-f2})c = \left(1 - \frac{f_1^2}{f_2^2}\right) I_{1,R}^S + (\alpha_1^S - \alpha_2^S) + (\alpha_{1,R} + \alpha_{2,R}) + (\lambda_1 N_{1,R}^S - \lambda_2 N_{2,R}^S) \quad (4b)$$

where:

- $I_{1,R}^S$ – slant ionospheric delay [m];
- f_i, λ_i – carrier waves frequencies [Hz] and wavelength [m], respectively;
- $\alpha_{i,R}, \alpha_i^S$ – (absolute) receiver- and satellite instrumental delays of the carrier phase observables, including initial phase bias [m];
- $\beta_{i,R}, \beta_i^S$ – (absolute) receiver- and satellite instrumental delays of the code-phase observables, including initial phase bias [m];
- $(\alpha_{1,R} - \alpha_{2,R})$ – receiver between-frequency bias [m];
- $(\alpha_1^S - \alpha_2^S)$ – satellite between-frequency bias [m].

The geometry (non-dispersive) terms in the observational equations (orbit, station coordinates, clock corrections, tropospheric refraction) cancel out. The ionospheric term, carrier-phase ambiguities and hardware delays remain.

Relations between the absolute instrumental biases in equations (4a) and (4b) and the inter-frequency (differential) instrumental biases [s] can be described by the following two relations:

$$\text{DCB}_{f_1-f_2,R} = \frac{\beta_{1,R} - \beta_{2,R}}{c} \text{ and } \text{DCB}_{f_1-f_2}^S = \frac{\beta_1^S - \beta_2^S}{c} \quad (5a)$$

$$\text{DPB}_{f_1-f_2,R} = \frac{\alpha_{1,R} - \alpha_{2,R}}{c} \text{ and } \text{DPB}_{f_1-f_2}^S = \frac{\alpha_1^S - \alpha_2^S}{c} \quad (5b)$$

After substituting (5a) into (4a) and (5b) into (4b), observation equations for estimation of ionospheric delay measurements [m] read:

$$\begin{aligned} (\delta\Delta t_{g,f_1-f_2})c &= \left(1 - \frac{f_1^2}{f_2^2}\right) I_{1,R}^S = P_{GF,R}^S + \\ &- c \left(\text{DCB}_{f_1-f_2}^S + \text{DCB}_{f_1-f_2,R}\right) \text{ [m]} \end{aligned} \quad (6a)$$

$$\begin{aligned} -(\delta\Delta t_{ph,f_1-f_2})c &= \left(1 - \frac{f_1^2}{f_2^2}\right) I_{1,R}^S = L_{GF,R}^S + \\ &- c \left(\text{DPB}_{f_1-f_2}^S + \text{DPB}_{f_1-f_2,R} + \lambda_{GF} N_{GF,R}^S\right) \text{ [m]} \end{aligned} \quad (6b)$$

where: $\lambda_{GR} N_{GF,R}^S = (\lambda_1 N_{1,R}^S - \lambda_2 N_{2,R}^S)$ is the geometry free carrier phase ambiguity.

Substituting the constant term in equation (2a) with its numerical value and conversion to TEC units, gives:

$$\frac{c}{40.30} \frac{f_1^2 f_2^2}{f_2^2 - f_1^2} = B = -2.854 \cdot 10^{25} \text{ [s]} \quad (7)$$

and insertion of (6a) into (2a) gives the following measurement model for determination of the sTEC from code-phase measurements:

$$\begin{aligned} \frac{1}{B} \text{sTEC}_{g,R}^S(t_j) &= \\ &= \left(\frac{1}{c} P_{GF,R}^S - \text{DCB}_{f_1-f_2}^S - \text{DCB}_{f_1-f_2,R}\right) \text{ [s]} \end{aligned} \quad (8a)$$

In a similar way, after inserting (6b) into (2b), the measurement model for sTEC from the carrier-phases reads:

$$\begin{aligned} -\frac{1}{B} \text{sTEC}_{ph,R}^S(t_j) &= \\ &= \left(\frac{1}{c} L_{GF,R}^S - \text{DPB}_{f_1-f_2}^S - \text{DPB}_{f_1-f_2,R}\right) + \\ &- \frac{1}{c} \lambda_{GF} N_{GF,R}^S \text{ [s]} \end{aligned} \quad (8b)$$

The algorithm for determination of differential code bias of the GNSS receiver is based on equation (8a). The equation has already been used by few authors (e.g. Coco et. al., 1991; Arikan et. al., 2008). The known parameters are:

- $P_{GF,R}^S$ – ionospheric observable derived from the code measurements (biased);
- $\text{DCB}_{f_1-f_2}^S$ – DCB for the satellite, which can be taken from the Centre for Orbit Determination in Europe, Bern (CODE);
- $\text{sTEC}_{ph,R}^S(t_j)$ – interpolated vTEC using Global Ionospheric Map (GIM) for the time and the place of observation and converted to its sTEC using one of the mapping functions, and the unknown DCB of the receiver can be estimated.

There are two important differences between the observables. The instrumental noise of the code-phase measurements is rather high: it is of order 30 cm for P-code and 3 m for C/A-code observables. The carrier-phase instrumental noise is only of order 3 mm, but the measurements are ambiguous. For this reason, simple approaches are often used for single receiver applications, e.g. for a simple point positioning. One of the earliest methods was proposed by Hatch (Hatch, 1982). He published an algorithm for smoothing of code observations with carrier phase ones. Recently, mainly for monitoring of the ionosphere, a group of “levelling” methods have been proposed. These methods are based on “shifting” of the carrier-phase connected arcs to the level of the code-arc and are known as “carrier phase levelling”. In this study, we used the second approach,

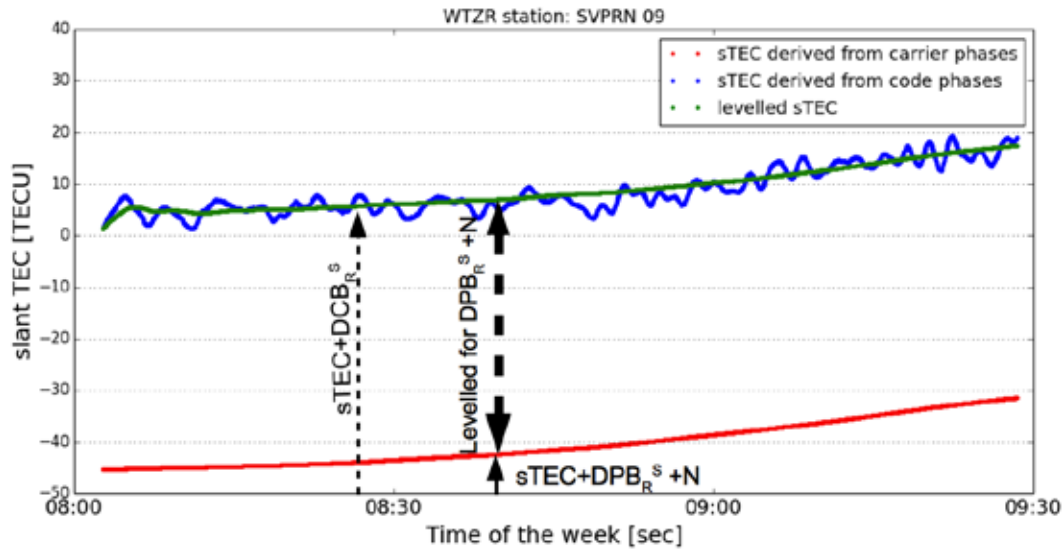


Figure 2. Levelling of the carrier-phase observations reduces the noise of code observations

as did a number of other authors estimating on-site TEC. The levelling technique we implemented here was described in Jakowski et al. (Jakowski et al., 2012). The following basic equation for estimation of the $DCB_{R,f1-f2}$, using code and carrier phases, is obtained:

$$sTEC_g = B \left(P_{GF,R,levelled}^S - DCB_{f1-f2}^S - DCB_{R,f1-f2} \right) \quad (9)$$

The DPB (differential carrier-phase bias) in equation (8b) has been accumulated together with the carrier-phase ambiguity (see Figure 2). The smoothing and levelling approaches are suitable for carrier-phase cycle slips. They have to be detected, and the observations should be corrected. However, the process of cycle slips detection is much more reliable than detection + correction. For this reason, it is strongly suggested to restrict the pre-processing algorithms to cycle slip detection only, to flag the related observational epochs and to re-initialise the smoothing (or levelling) algorithms. The data used for validation of the algorithm presented here have been pre-processed and flagged with our academic software suite TUB-NavSolutions.

Validation of the algorithm for estimation of GPS receiver differential code bias in a single station mode

GPS data from the Wettzell station have been selected for validation of the algorithm, because at the CODE there are also available DCBs for receivers contributing to the IGS global network.

Single layer ionospheric maps provide vertical (in the local zenith direction) values of the TEC (vTEC). The vTECs have been calculated using GIM available at the CODE. However, in equation (9) the sTECs appear. These must be converted to vTECs, or interpolated vTECs must be converted to slant values. Projection of the measured sTEC to an appropriate (equivalent) vertical TEC value is a function of elevation angle E of the line-of-sight and reads:

$$sTEC(E) = vTEC(E) \cdot M(E) \quad (10)$$

There are several ionospheric mapping functions commonly used. One of the earliest is the *standard geometric ionospheric mapping function* originally proposed by Mannucci et al. (Mannucci et al., 1999). However, we selected the modified single-layer

Table 1. Comparison of the estimated receiver DCBR,f1-f2 for IGS station Wettzell

Satellite PRN	Calculated DCBR,f1-f2 [ns]	rms [ns]	Local time	Duration	Maximal elevation angle
18	14.728	±0.461	00:13:31 – 00:51:31	00h 38m 00s	52°
19	15.880	±0.549	01:32:31 – 04:49:31	03h 17m 00s	81°
04	15.421	±0.217	02:51:31 – 06:31:24	03h 39m 53s	87°
11	16.137	±0.213	03:23:00 – 06:30:54	03h 07m54s	80°

Our average: 15.541 ±0.535 ns; our average without SV18: 15.813 ±0.296 ns; $DCB_{R,f1-f2}$ taken from IONEX: the same day: 15.297 ns, monthly value: 15.308 ns

mapping function (MSLM), because it is used in CODE-GIM for generation of ionospheric maps.

The GPS observations have been taken for 17 March 2015. Only selected arcs of satellites around local midnight and elevation angle higher than 40° have been processed. The first results are presented in Table 1.

Conclusions

Our average DCB is close to the reference value; however, the RMS is a little high. Certainly, the above data from only one day and four satellites are not sufficient for a good statistical conclusion. However the results are satisfactory. The experiments will be continued to provide users (e.g. surveyors) with an operational software tool.

Acknowledgments

Part of this research has been supported by the German Federal Ministry of Education and Research (BMBF) listed under the support code 16N036426 (iP4GNSS/REIMANT).

References

1. ARIKAN, F., NAYIR, H., SEZEN, U. & ARIKAN O. (2008) *Estimation of single station interfrequency receiver bias using GPS-TEC. Radio Science* 43:RS4004.
2. COCO D.S., COKER, C.E., DAHLKE, R. & CLYNCH J.R. (1991) Variability of GPS satellite differential group delay biases. *IEEE Transactions on Aerospace and Electronic Systems* 27 (6). pp. 931–938.
3. GALAS R., REIGBER, Ch., BURGHARD, W. & ROMSTEDT R. (2003) *GPS Permanent Deformation Monitoring Array on Popocatepetel Volcano*. Internal report and poster presentation, GFZ-Potsdam.
4. HARTMAN G.K. & LEITINGER R. (1984) Range errors due to ionospheric and tropospheric effects for signal frequencies above 100 KHz. *Bulletin Geodesique* 58 (2). pp. 109–136.
5. HATCH R. (1982) The synergism of GPS code and carrier measurements. *Proceedings of the International Geodetic Symposium on Satellite Doppler Positioning*, Las Cruces, New Mexico. pp. 1213–1231.
6. HOFMANN-WELLENHOF, B., LICHTENEGGER, H. & WASLE E. (2008) *GNSS Global Navigation Satellite Systems*.
7. JAKOWSKI, N., MAYER, C., HOQUE, M.M. & WILKEN, V. (2012) Total electron content models and their use in ionosphere monitoring. *Radio Science* 46.
8. KLOBUCHAR J.A. (1996) Ionospheric Effects on GPS. In *Global Positioning Systems: Theory and Applications 1*. Eds: B.W. Parkinson and J.J. Spilker, Jr., American Institute of Aeronautics and Astronautics, pp. 547–568.
9. MANNUCCI, A.J., IJIMA, B.A., LINDQUISTER, U.J., PI, X., SPATKS, L. & WILSON, B.D. (1999) GPS and Ionosphere. *Revised Submission to URSI Reviews of Radio Science*. JPL. March 1999 edition.